



Enhanced wound healing promotion by immune response-free monkey autologous iPSCs and exosomes vs. their allogeneic counterparts

Meng Lu, Peng Lu, Ming Xu, Xiaokai Wang, Anfeng Cui, Yijun Li, Xinhong Wang, Dan Meng, Ning Sun, Meng Xiang*, Sifeng Chen*,¹

Department of Physiology and Pathophysiology, School of Basic Medical Sciences, Fudan University, Shanghai 200032, China

ARTICLE INFO

Article history:

Received 25 October 2018

Received in revised form 8 February 2019

Accepted 4 March 2019

Available online 26 March 2019

Keywords:

Allogeneic stem cells
 Autologous stem cells
 Wound healing
 Non-human primate
 Yamanaka factors
 Immune response
 Exosomes
 Stem cell therapy
 Teratoma

ABSTRACT

Background: Comparing non-inbred autologous and allogeneic induced pluripotent stem cells (iPSCs) and their secreted subcellular products among non-human primates is critical for choosing optimal iPSC products for human clinical trials.

Methods: iPSCs were induced from skin fibroblastic cells of adult male rhesus macaques belonging to four unrelated consanguineous families. Teratoma generativity, host immune response, and skin wound healing promotion were evaluated subsequently.

Findings: All autologous, but no allogeneic, iPSCs formed teratomas, whereas all allogeneic, but no autologous, iPSCs caused lymphocyte infiltration. Macrophages were not detectable in any wound. iPSCs expressed significantly more MAMU A and E of the major histocompatibility complex (MHC) class I but not more other MHC genetic alleles than parental fibroblastic cells. All topically disseminated autologous and allogeneic iPSCs, and their exosomes accelerated skin wound healing, as demonstrated by wound closure, epithelial coverage, collagen deposition, and angiogenesis. Allogeneic iPSCs and their exosomes were less effective and viable than their autologous counterparts. Some iPSCs differentiated into new endothelial cells and all iPSCs lost their pluripotency in 14 days. Exosomes increased cell viability of injured epidermal, endothelial, and fibroblastic cells in vitro. Although exosomes contained some mRNAs of pluripotent factors, they did not impart pluripotency to host cells.

Interpretation: Although all of the autologous and allogeneic iPSCs and exosomes accelerated wound healing, allogeneic iPSC exosomes were the preferred choice for “off-the shelf” iPSC products, owing to their mass-production, with no concern of teratoma formation.

Fund: National Natural Science Foundation of China and National Key R&D Program of China.

© 2019 Published by Elsevier B.V. This is an open access article under the CC BY-NC-ND license (<http://creativecommons.org/licenses/by-nc-nd/4.0/>).

1. Introduction

Induced pluripotent stem cells (iPSCs) comprise embryonic-like stem cells reprogrammed from adult somatic cells. iPSC technology has opened up unique opportunities for developing patient-specific cell therapies and mechanistic studies because of their limitless self-renewal capacity and ability to become any somatic cell type within the body [1–3]. As patient-specific autologous iPSC lines are genetically identical to the recipient individual (the same patient), iPSCs and their derivatives are therefore not expected to be immune rejected, unlike allogeneic cells and organ transplants. In comparison, allogeneic iPSCs

and their derivatives can be mass produced and the immune rejection by recipient animals can be reduced through use of immune inhibitors to some extent. Conversely, autologous iPSCs are patient-specific and cannot be mass-produced; rather, they have to be prepared individually. Thus, it is important to determine the tradeoff between time and workload of individualized autologous iPSC generation and immune rejection of allogeneic iPSCs and their derivatives.

Recipient immune responses to transplanted inbred syngeneic and allogeneic iPSCs as well as their derived cells have been observed [4–7]. For example, inbred iPSCs were induced from a separate animal of the same inbred line instead of the particular animal receiving the iPSC transplant, whereas allogeneic iPSCs were induced from cells of leukocyte antigen-mismatched inbred animals including minipigs, rather than allogeneic non-inbred animals [7]. Notably, immune rejection to both inbred syngeneic and allogeneic iPSCs was found [8]. However, inbred syngeneic animals are not fully genetically identical; thus,

* Corresponding authors at: Department of Physiology and Pathophysiology, School of Basic Medical Sciences, Fudan University, Shanghai 200032, China.

E-mail addresses: xmeng@shmu.edu.cn (M. Xiang), chen1216@fudan.edu.cn (S. Chen).

¹ Lead Contact.

Research in context

Evidence before this study

Although induced pluripotent stem cells (iPSCs) provide great therapeutic opportunities, it is yet to be widely translated into clinical practice mainly due to the concerns of potential teratoma (a benign tumour) formation and host immune response against iPSCs. Using 53 experimental conditions and diseased models, we recently demonstrated that intravenously or topically disseminated iPSCs lose pluripotency in three days and do not form teratoma. Thus, direct application of iPSCs in vivo is feasible and can be safe.

Patient-specific autologous iPSCs are genetically identical to that of the recipient individual (the same animal as recipient), but needs to be prepared individually. In comparison, allogeneic iPSCs can be produced in large-scale, but may be immune-rejected. Immune-rejection of both syngeneic and allogeneic iPSCs has been reported. However, immune-rejection associated with actual autologous iPSC treatment (the same animal as recipient) has not been examined under foreign antigen-free environment, especially in non-human primates, to ensure a safe and effective iPSC therapy. Determination of the trade-off between time or workload of individualized autologous iPSC generation and immune-rejection of allogeneic iPSCs and their derivatives is important.

Stem cell therapy includes providing functional parenchymal cells and promoting angiogenesis and paracrine response. Exosomes, which are secreted by cells and deliver clustered molecules of related functional groups across cells, represent an attractive and alternative tool to stem cell-based therapy.

Wound healing impairment, especially in refractory diabetic skin wounds, constitutes a common and challenging clinical problem for which effective treatment is currently unavailable. Owing to the open exposure and easy visibility of skin wounds, they represent an ideal candidate for initial clinical trials, since they allow rapid observation and teratoma removal, if any.

Added value of this study

Cross-examination using iPSCs induced from fibroblastic cells of rhesus macaque, belonging to four unrelated consanguineous families, showed that all allogeneic, but no autologous, iPSCs and exosomes caused immune response. iPSCs expressed significantly more MAMU A and E of major histocompatibility complex (MHC) class I than their parental fibroblastic cells. However, other major MHC I and II genetic alleles were not detectable in the iPSCs. Allogeneic iPSCs and their exosomes were less viable than their autologous counterparts in the wounds and were less effective in promoting wound healing. In particular, there was no statistically significant difference between autologous iPSCs and their exosomes or between allogeneic iPSCs and their exosomes. Only a few administered iPSCs differentiated into new endothelial cells and all iPSCs lost their pluripotent state in 14 days. No evidence showed iPSCs differentiating into epidermal cells. Exosomes increased cell viability of all three major cell types, epidermal, endothelial and fibroblastic, responsible for skin wound healing in vitro. Exosomes did not impart pluripotency to host cells.

Implications of all the available evidence

Our data indicate that lack of immune response to actual autologous iPSCs may be responsible for the greater viability and effectiveness of autologous iPSCs and exosomes in promoting wound healing compared to that of their allogeneic counterparts. The failure of autologous iPSCs to cause T and B lymphocyte infiltration may not be due to their incapability of presenting antigen episodes.

Lack of epidermal differentiation and difference between autologous iPSCs and their exosomes or that between allogeneic iPSCs and their exosomes indicate that iPSCs promote wound healing mainly by secreting therapeutic substances. In other words, exosomes can be an alternative for iPSCs.

The fact that all administered iPSCs lost pluripotent state in 14 days demonstrated that the injected iPSCs do not survive as quiescent stem cells, hence ensuring long-term safety of the cells. Our previous long-term study had suggested that the injected iPSCs survive in injured organs for 28–90 days. Mal-differentiation of iPSCs into unwanted cells that are replaced by the body periodically, such as mislocated or misoriented endothelial cells and epidermal cells, are not as worrisome since they will eventually disappear after their natural life span. Thus, providing long-lasting renewable cells is not the goal of iPSC therapy for organs, such as lungs, liver, kidney and skin, in which epithelial cells serve as parenchymal cells.

Although allogeneic iPSCs and exosomes were not as viable and effective as their autologous counterparts, they were sufficient in promoting wound healing. Overall, allogeneic iPSC exosomes may be the preferred choice for “off-the shelf” iPSC product, considering their mass-production, with minimal safety concerns.

the extent of leukocyte antigen-mismatch may differ from the nature of human allogeneic cells, with variations in non-leukocyte antigens also potentially being present.

To accelerate the potential of iPSC-based cellular therapies, the immune rejection associated with actual autologous iPSC treatment (the same animal as recipient) should be examined, especially in non-human primates, to ensure safe and effective iPSC therapy. Morizane et al compared autologous and allogeneic transplantation of iPSC-derived neural cells in the brain of purpose-bred cynomolgus monkeys directly [9]. They found that the autologous iPSC-derived neurons elicited some immune response in the brain. The allogeneic iPSC-derived neurons were less survival and caused a significantly more severe acquired immune response. However, the cells were injected in the suspension of the neurobasal medium with B27 (medium supplement) added with glial-cell-line-derived neurotrophic factor and brain-derived neurotrophic factor. For the monkeys, B27 contained large amount of xenogeneic protein antigens. The added glial-cell-line-derived neurotrophic factor and brain-derived neurotrophic factor are also xenogeneic protein antigens for monkeys. Thus, the immune response in the injection sites of autologous iPSC-derived neurons may be caused by these xenogeneic antigens. Hong et al. reported that undifferentiated monkey autologous iPSCs form teratomas (encapsulated benign tumors with normal cells of all three germ layers) along with the presence of immune/inflammatory cells [10]. Because the immune/inflammatory cells were found in mature teratomas containing intact teratoma structures without evidence of significant tissue damage, it was considered likely that the immune/inflammatory cells represented iPSC-differentiated cells, as lymphocytes can be prepared from iPSCs [11]. Accordingly, the teratoma assay is not the best model to test iPSC

immunogenicity. A better approach would be to sequentially immunize the recipient animals with iPSCs followed by secondary iPSC injection at a different site, harvest the injected cells along with surrounding tissue prior to mature teratoma generation, and examine the immune response.

It is also possible for a recipient to develop an immune response against iPSCs induced from his/her own cells because iPSCs may contain some proteins that express transiently during embryo development and disappear before the immune system of the body is developed. The team led by J. Wu found that irradiated iPSC vaccines elicited an anti-tumour response in inbred syngeneic murine cancer models [12]. However, immunogenicity does not necessarily translate into immune rejection, because the cellular membrane may prevent the intracellular antigens of living cells from being targeted by the immune system. Thus, as long as pre-existing immunogenicity does not target extracellular antigen presentation episodes of autologous cells, iPSCs may survive and eventually differentiate into lineage-specific cells under induction by the microenvironment. Similarly, allogeneic iPSCs may also survive longer than expected. Several studies have shown that iPSC-derived terminally differentiated cells did not elicit a significant immune response [13,14]. However, studies using iPSC-derived stromal cells are only able to examine immune responsiveness to the specific cell type; the antigenicity of most cell types is not examined. Thus, using un-differentiated iPSCs may reveal a broader image of the immune response to transplanted autologous iPSCs.

The mechanisms of stem cell therapy include providing functional parenchymal cells, promoting angiogenesis and paracrine response. The development of numerous non-integrating virus-based iPSC induction and derivation approaches has removed most hurdles of *in vivo* iPSC application [15,16]. Nevertheless, the potential of iPSCs and their differentiated progeny to form teratomas upon transplantation still exists. Thus, direct *in vivo* application of iPSCs is not currently recommended. In comparison, exosomes, which comprise nano-sized membrane complexes secreted by cells as cargos for cell-cell communication, represent an attractive alternative approach to stem cell-based therapy [17,18]. Exosomes deliver clustered molecules of related functional groups between cells. Although serving as an efficient form of paracrine signalling, exosomes are not proliferative and, therefore, do not form teratoma-like tumour masses. However, the therapeutic efficiency and durability between exosomes isolated from autologous and allogeneic iPSCs have not been previously compared.

It is critical to assess the safety and efficiency of iPSC-based therapies in a clinically relevant model in the presence of an intact immune system. Nonhuman primates (NHPs), such as rhesus macaque, are similar to humans in size, behaviour, physiology, structure and function of organs, biochemistry, and immune system [10,19,20]. Often NHPs are more efficient and useful for evaluating new proof-of-concept therapeutics prior to their first-in-human trials than rodents and/or other species. Research on NHPs offers unique opportunities to test the feasibility, disadvantages, and advantages of stem cell-based therapeutic interventions that may later be applied in the clinic.

Wound healing impairment, especially refractory diabetic skin wounds, constitutes a common and challenging clinical problem for which effective treatment is currently unavailable. Notably, foot ulceration is the most frequently recognized complication of diabetes [21]. According to 2015 data of the International Diabetes Federation, each year, 9.1 million to 26.1 million people with diabetes develop foot ulcers worldwide, leading to nonhealing ulcers, infection, and amputation in many cases. Cell therapies, such as autologous bone marrow-derived mesenchymal stem cells (MSCs), and fibroblast lineages have been applied on different wounds in various studies [22,23]. iPSCs have advantages in cell therapy over other stem cells in availability, propagation and pluripotency [1–3,24]. Comparing the effects of autologous and allogeneic iPSCs, as well as their exosomes, will provide value in determining the optimal kind of iPSC for use. Moreover, owing to the exposure and easy observation of skin wounds, it is straightforward to

monitor the effect of applied stem cell therapy. In addition, as teratomas comprise benign (non-metastatic) tumors, skin wounds represent an ideal candidate for initial clinical trials as they allow rapid observation and removal of teratomas if they should occur.

Based on these considerations, in the present study we established four iPSC lines from four rhesus macaques to compare the immune responses and therapeutic effects of transplanted autologous and allogeneic iPSCs as well as their derived cellular products (exosomes), along with their relative safety and efficacy.

2. Materials and methods

2.1. Animals

The animal protocols were approved by the Animal Care Committee of the Fudan University Shanghai Medical College (Approval Nrs. 20080411, 20120302-103 and 201504270-001) in accordance with the Guide for the Care and Use of Laboratory Animals (National Research Council of the United States). All procedures involving animals were performed in accordance with institutional guidelines and permission of the Ethics Committee at the Fudan University Shanghai Medical College. Non-obese diabetes/severe-combined immunodeficient (NOD/SCID) mice were purchased from Shanghai SLAC Laboratory animal C. Ltd. (Shanghai, China). Four adult male macaques from unrelated consanguineous families (all were farm-raised 3rd generation) were purchased from the Dongwu Experimental Monkey Farm (Ningbo, China). They were born in March and April of 2006 and housed in an animal laboratory at the Fudan University affiliated Shanghai Public Health Clinical Centre (Shanghai, China) since being purchased in 2009. Aside from routine examination, they never mated with female macaques and did not receive any previous treatment. Their tag numbers were 200603005, 200603009, 200604011 and 200604013.

2.2. Generation and culture of iPSCs

As described previously [16], macaque skin fibroblasts were transfected with a Sendai virus (Thermo Fisher Scientific) mixture at multiplicities of infection (MOIs) of 5, 5, and 3 for KOS (OCT4/SOX2/KLF4), hc-Myc, and hKLF4, respectively, at 37 °C in air containing 5% CO₂ for 40 min. The cells were then plated in Matrigel-coated 6-well plates and cultured in DMEM with 10% FBS and 1 mM valproic acid for 3–4 days until significant morphological changes were observed. Then, the cells were trypsinised and re-plated onto fresh mitomycin C-treated mouse embryonic fibroblastic cells (MEFs) at a 1:6 ratio. MEFs pre-treated with mitomycin C served as feeder cells. The medium was replaced with knockout serum replacement (KSR) medium containing 85% DMEM/F12 (DF12), 15% KSR (Thermo Fisher Scientific), 1 mM L-glutamine, 0.1 mM non-essential amino acids, 0.1 mM β-mercaptoethanol, and 5 ng/ml basic fibroblast growth factor (bFGF, Thermo Fisher Scientific). The medium was changed every day until the colonies grew sufficiently large to be picked up.

The clone-like macaque iPSCs were passaged every 4–6 days with collagenase IV and re-plated onto mitomycin C- pre-treated MEFs. The induced cells were demonstrated as iPSCs by alkaline phosphatase (AP) staining, quantitative PCR and immunohistochemical staining for pluripotency markers, and teratoma generation assay using cells of passage 10.

2.3. Macaque iPSC expansion

For macaque iPSC expansion, clone-like macaque iPSC masses were manually cut into smaller cell masses with a 10-μl pipette tip and transferred onto fresh MEFs. The macaque iPSCs were passaged every 4–6 days with collagenase IV (1 mg/ml) at 37 °C for 15 min and re-plated onto fresh MEFs. Cells of passage 18 and beyond were used for

experiments to minimize the heterogeneity among cells from different animals because studies have shown that the differences in epigenetic inheritance among iPSCs from different animals become negligible after passage 16 [25]. Prior to being used for treatment and exosome isolation, the cells were cultured on plates coated with Matrigel (Matrigel™, BD Bioscience, Franklin Lakes, NJ) using the iPSC medium mTeSR™1 (STEMCELL Technologies Inc., Vancouver, Canada) but free of feeder cells (MEFs) for two generations.

2.4. Experimental timeline

The order of the experiments (Supplementary Fig. 1 and Supplementary Table 1) was as follows: 1) Isolation of macaque skin fibroblastic cells, and induction and identification of iPSCs from all four macaques. 2) Parallel comparison of teratoma formation over 28 days after subcutaneous injection with Matrigel between autologous and allogeneic iPSCs. Each macaque received four parallel subcutaneous injections with their own autologous iPSCs and allogeneic iPSCs from the other three macaques, respectively, in right axilla. The cells were suspended in 1:1 mixture of phosphate buffered saline (PBS) and Matrigel solution. The dose was 1×10^7 cells per spot. After finishing 28-day teratoma observation, the injections were repeated in the left axilla. 3) Comparison of T lymphocyte infiltration at three days after subcutaneous injection. The injected cells of second injection and surrounding tissue were harvested three days after injection for observation of immunogenicity. Because of limited axilla space, iPSCs from three macaques other than the macaque receiving the cells were equally mixed and served as allogeneic iPSCs. The dose of autologous or mixed allogeneic iPSCs was 1×10^7 cells per spot. 4) Comparison of the effects of autologous and allogeneic iPSCs and their exosomes toward accelerating wound healing. Each macaque was received 24 skin punch wounds on the back. The size of the wound was four millimetres. The wounds of each macaque were designated to receive iPSCs and their exosomes from all four macaques. Each treatment was performed in triplicate in order to biopsy samples of each treatment on day 3, 7, and 14 after wound punching.

2.5. Alkaline phosphatase detection

AP staining was performed using an AP detection kit (Sigma-Aldrich, St. Louis, MO) according to the manufacturer's instructions.

2.6. Western blotting for CD3, CD20, CD68, OCT4, SOX2, SSEA4, ALIX, and TSG101

The tissue containing iPSCs injected for immunogenicity examination was harvested three days after injection. Tissue lysates were separated by sodium dodecyl sulphate-polyacrylamide gel electrophoresis (12% resolving gel) and transferred to a polyvinylidene difluoride membrane. The membrane was blocked with donkey serum, incubated with primary and secondary antibodies subsequently. The primary antibodies were rat monoclonal anti-CD3, rabbit monoclonal anti-CD20, mouse monoclonal anti-CD68/SR-D1, rabbit polyclonal anti-OCT4 or TSG 101, and mouse monoclonal anti-SOX2, SSEA4 or ALIX. The secondary antibodies were Peroxidase AffiniPure Donkey Anti-rat, Anti-rabbit, or Anti-mouse IgG (H + L) (Jackson ImmunoResearch Inc., West Grove, PA). Detail information of the antibodies was shown in Supplementary Table 2. The immunoreactive bands were visualized using enhanced chemiluminescence substrate.

2.7. Reverse transcriptase-PCR and real-time PCR for pluripotency markers

Total RNA was extracted from cultured iPSCs or exosomes using TRIzol Reagent. RNA concentrations and purities were determined using a Nanodrop instrument at wavelengths of 260/280 nm. cDNA was synthesized from 1 µg of total RNA using superscript III (Thermo

Fisher Scientific) according to the manufacturer's instructions. The cDNA was diluted with DNase-free water to a concentration of 10 ng/µl. Real time PCR was performed in a Bio-Rad iQ Real-Time PCR Detection System (Bio-Rad, Hercules, CA) using the IQ SYBR Green SuperMix with the following thermal cycles: initial denaturation 95 °C for 5 min, 40 cycles of 20 s at 95 °C, 45 s at 57 °C, and 30 s at 72 °C. Analyses of mRNA levels of target genes were normalized to *GAPDH* as the internal control and expressed relative to the quantity of the control group. The primers are shown in supplemental table of key resources (Supplementary Table 2).

2.8. Reverse transcriptase-PCR and real-time PCR for genetic alleles of MHC I and II

Total RNA was extracted from the cultured iPSCs and corresponding skin fibroblastic cells were used for iPSC induction. Expression of genetic alleles, including MAMU A, B, and E of MHC class I and MAMU DQA, DQB, DRB, DPA, and DPB of MHC class II was measured using quantitative real-time PCR with conditions same as in the measurement of pluripotent makers. The primers are shown in Supplementary Table 2.

2.9. Immunofluorescence for pluripotency markers in iPSCs

Cells were fixed in 4% paraformaldehyde at room temperature for 20 min, rinsed with PBS, and blocked by 5% donkey serum at room temperature for 60 min. For cytoplasmic protein staining, 0.3% Triton X-100 was added for permeabilisation. Cells were then incubated with primary antibodies against OCT4, Nanog and SSEA4 (Supplementary Table 2) diluted in 5% donkey serum at 4 °C overnight, respectively. Cells were washed and exposed to secondary antibodies at room temperature for 60 min. The cells were finally stained for the nuclei with 1 µg/ml blue fluorescent dye, 4', 6-diamidino-2-phenylindole, dihydrochloride (DAPI).

2.10. Isolation and identification of exosomes

Exosomes in cell culture supernatants were isolated using a combination of exosome purification kit (ExoQuick kit, System Biosciences Inc., Palo Alto, CA) and ultracentrifugation assay. Dead cells and large cell debris were removed by centrifuging the culture supernatant at 200 g for 10 min and then at 2000 g for 20 min. This media was then concentrated by centrifugation for 10 min at 5000 g in a pre-rinsed 100 kDa MWCO Millipore Ultrafree-15 capsule filter to a desired volume. An ExoQuick kit was then used to purify exosomes by precipitating them from the concentrated cell culture supernatant. The exosomes were further purified by ultracentrifugation (100,000 g). The exosomes were identified by transmission electron microscopy and nanoparticle tracking analysis.

2.11. Transmission electron microscopy

For transmission electron microscopy, 20 µl of PBS containing purified exosomes was placed on formvar carbon-coated 200-mesh copper electron microscopy grids, incubated for 5 min at room temperature, and subjected to standard uranyl acetate staining. Electron micrographs were recorded using a transmission electron microscope (FEI Tecnai G2, Hillsboro, OR). Micrographs were used to quantify the diameter of exosomes.

2.12. Nanoparticle tracking analysis (NTA)

The particle number and concentration of exosomes were assessed using the Nanosight LM10-HS system (Malvern Instruments Ltd., Malvern, UK) equipped with a 488 nm laser at 25 °C. Samples were diluted to an acceptable concentration according to the manufacturer's recommendations and introduced into the chamber manually. Each

experiment was carried out in triplicate and the instrument laser chamber was cleaned thoroughly between samples.

2.13. Teratoma formation in immune-deficient mice

As described previously [16], to confirm the pluripotency and capability to form teratomas, 5×10^6 macaque iPSCs, in a volume of 100 μ l (50 μ l medium and 50 μ l Matrigel) were harvested and subcutaneously injected into NOD/SCID mice. Teratomas formed 8 weeks later. Mice were executed and tumors were dissected, fixed with 4% paraformaldehyde, and processed into paraffin sections. The tissues were stained with haematoxylin and eosin to determine whether teratomas contained tissues from all three germ layers.

2.14. Full-thickness excisional wound models

For major surgeries, the animals were injected with atropine sulphate (0.05 mg/kg). At 30 min after atropine sulphate injection, the monkeys were anesthetized by intra-muscular injection of anaesthetic mixture (0.15 ml/kg body weight). Each ml of the mixture contained 33.33 mg ketamine hydrochloride, 40 mg xylazine, 2.67 μ g dihydroetorphine, and 1.67 mg haloperidol. Macaques were anesthetized before full-thickness excision wounds were created. The macaque dorsal skin was prepared by removing hair with depilatory cream. Full-thickness excision wounds were created by excising the full-thickness skin in the mid-back with a four millimetre biopunch (FRAY).

2.15. Cell and exosome labelling

All macaque iPSCs and exosomes were labelled with the fluorescent dye, PKH26 Red, using a Fluorescent Cell Linker Kit (Sigma-Aldrich) prior to being applied to wound surfaces. Cells were washed three times with PBS, incubated with collagenase IV (1 mg/ml), and re-suspended in 500 μ l diluent C of the cell linker kit in a 1.5 ml Eppendorf tube. PKH26 Cell Linker reagent (2 μ l) diluted with another 500 μ l diluent C was added into the cell or exosome suspension, which was then incubated at room temperature for 5 min. After washing with PBS, the cells and exosomes were suspended in PBS.

2.16. iPSC and exosome application

When using iPSCs for treatment, a bolus of 4.6×10^4 iPSCs (autologous or allogeneic) in 20 μ l were topically applied onto the surface of the macaque skin wound. For exosomes, a bolus of 50 μ g exosomes (autologous or allogeneic) was topically placed onto the wound.

2.17. Wound closure evaluation

Images of the wounds designated for 14-day observation were captured on day 0, 3, 7, 10, and 14. Wound areas were quantitated by the ImageJ software (National Institutes of Health, Bethesda, MD). The wound closure were calculated by using the following equation: wound closure (%) = (wound area on day 0 – wound area on the indicated day) \times 100%/wound area on day 0.

2.18. Wound sample processing

The wounds, together with 1.5–2 mm uninjured skin margins, were excised at 3, 7, and 14 days after wound injury. Each sample was divided into three pieces. For haematoxylin and eosin, Masson's trichrome, and immunochemical staining, a portion of the sample was fixed in 4% paraformaldehyde. Capillary density in the healing wounds was quantified by histological analysis of CD34-immunohistochemically stained sections. For demonstrating the existence of administered iPSCs or exosomes, a portion of the sample was embedded in OTC prior to

freezing for immunofluorescence analysis. The remaining piece was preserved in liquid nitrogen for extraction of RNA or protein.

2.19. Detection of iPSCs and exosomes in the wound biopsy

iPSCs or exosomes were labelled with PKH26 Red Fluorescent Cell Linker prior to in vivo administration. The wound and surrounding skin were collected and embedded in OTC prior to freezing. To identify the transplanted cells or exosomes in the wound, five micrometre thick cryo-sections were prepared. Sections were counterstained with DAPI. The red and blue fluorescence were captured in the same field under a fluorescence microscope (Leica Microsystems, Wetzlar, Germany) and merged.

2.20. Co-localization of administered iPSCs and new endothelial cells

Cryo-sections of skin tissue receiving PKH 26-labelled iPSCs were stained with mouse monoclonal anti-CD34 antibody (1:200 dilution; Abcam, ab8536) and Alexa Fluor 488 AffiniPure Donkey anti-Mouse IgG (Shanghai Yisheng Biological Technology Co., Ltd. Cat. 34106ES60) using immunofluorescent assay. Co-localization signals of CD34 and administered cells were photographed under a Leica fluorescence microscope (Leica).

2.21. Histopathologic analysis of skin wounds

Tissue biopsies from wounds designated for harvesting samples on day 3, 7, and 14 of wound injury were collected. For histopathologic evaluations, the specimens were fixed in 4% paraformaldehyde and processed for paraffin sections. Sections (five micrometre thickness) were cut and stained with haematoxylin and eosin. The slides were assessed under a light microscope (Leica) for epidermal thickness. The thicknesses of the epidermal areas formed were measured in five different places along the wound surface and the average of these areas was taken as the thickness of the epidermis.

2.22. Immunohistochemical staining for SSEA4, OCT4 and CD34

Paraffin sections were subjected to antigen retrieval with citrate buffer at 95 °C for 8 min, and incubated with 0.3% hydrogen peroxide for 15 min, 5% normal donkey serum for 1 h, primary antibodies, and HRP-conjugated donkey anti-mouse IgG secondary antibodies. The primary antibodies were mouse monoclonal anti-human SSEA4 (Thermo Fisher), mouse monoclonal anti-OCT3/4 (Abcam) and anti-CD34 antibodies (Abcam). Peroxidase activity was visualized using diaminobenzidine. Sections were counterstained with haematoxylin before observation. For the negative control, the primary antibody was replaced with 5% normal donkey serum. Dispersed iPSCs smeared on glass slides were stained and they served as additional positive and negative controls for SSEA4 and OCT4 staining. Images were captured with a Leica microscope.

2.23. Cell viability measurement in vitro

With approval from the Ethics Board of Fudan University and informed consent from participants, primary human umbilical vein endothelial cells (HUVECs) were obtained from three fresh umbilical cord veins of normal pregnancies. HUVECs were isolated by collagenase digestion, as described previously [26]. They were maintained in endothelial cell medium (ECM, ScienCell Research Laboratories, Carlsbad, CA). Cells between passages four and five were used for the experiments. Human dermal fibroblastic cells (HDF) and spontaneously transformed human keratinocyte cells (HaCaT), both from Shanghai Zhong Qiao Xin Zhou Biotechnology Co. Ltd. (Shanghai, China), were cultured in DMEM. All media were supplemented with 10% FBS and 1% antibiotics (penicillin/streptomycin; 100 U/ml). All

cells were incubated in a humidified incubator supplied with 5% CO₂ at 37 °C.

Effects of exosomes on cell viability were evaluated using the Cell Counting Kit-8 (CCK-8) (Dojindo Laboratories, Kumamoto, Japan) according to the manufacturer's instructions. Cells were seeded into 96-well plates at 1×10^4 cells/well and cultured for 24 h. They were treated with cisplatin (30 µg/ml) and autologous or allogeneic exosomes (20 µg/ml). Cells treated with PBS or cisplatin alone served as untreated and treated controls, respectively. Cell viability curves were constructed by measuring the amount of formazan dye generated by cellular dehydrogenase activity using a microplate spectrophotometer at a wavelength of 450 nm.

2.24. Incubation of macaque skin fibroblastic cells with iPSC-derived exosomes

Skin fibroblastic cells from the rhesus macaques were treated with iPSC exosomes for 4 h and 16 h, or 4 h with exosomes followed by 12 h without exosomes, or 16 h with exosomes followed by 24 h without exosomes. The exosomes were isolated from rhesus macaque iPSCs. The iPSC exosome concentration, used for the treatment, was 20 µg/ml. Fibroblastic cells and iPSCs cultured in iPSC exosome-free medium served as negative and positive controls, respectively. After treatment, the cells were harvested and used either for quantitative PCR (for mRNAs), or for immunofluorescence and Western blotting (for proteins) of pluripotent factors.

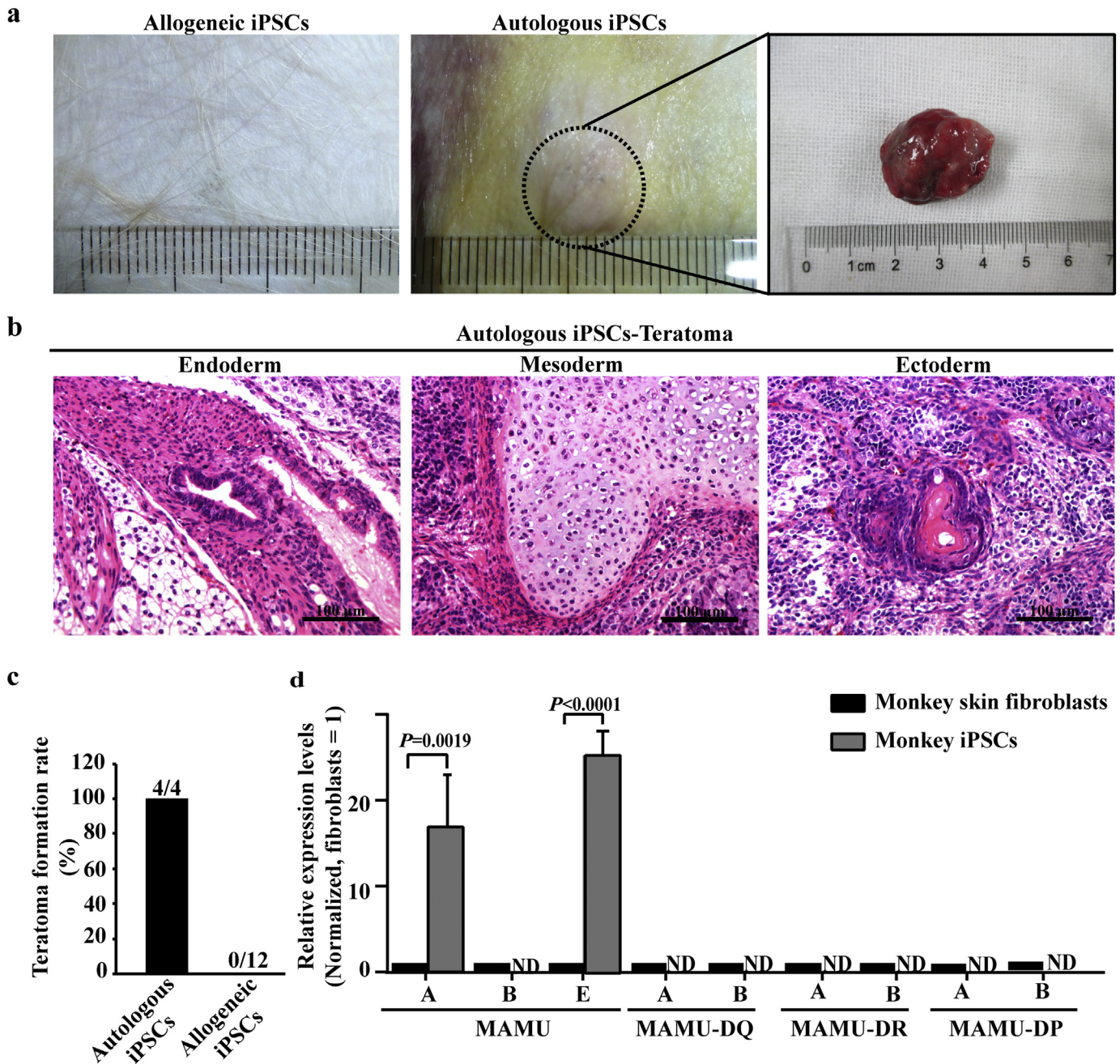


Fig. 1. Teratoma formation and expression of genetic alleles of major histocompatibility complex I and II in autologous and allogeneic macaque iPSCs. (a) Allogeneic iPSCs failed to generate teratomas. (b–f) Autologous iPSCs formed mature teratomas with three germ layers. (g) Teratoma generation rates of autologous and allogeneic iPSCs. (h) Expression of genetic alleles of the major histocompatibility complex I and II in monkey iPSCs and skin fibroblastic cells.

2.25. Masson trichrome staining of wounds

Masson trichrome staining was employed for quantitative evaluation of the effect of iPSC and exosome transplantation on collagen deposition during wound healing. Serial paraffin sections from the mid-portion of the wound were stained with Masson's trichrome according to the manufacturer's protocol. Photographs of each section were taken under a Leica microscope. Collagen deposition was analysed using ImageJ software (NIH) and calculated as follows:

Collagen area proportion (%) = accumulated positive area within Masson's stained wound / wound area \times 100%.

2.26. Quantitation and statistical analysis

The results are presented as the means \pm standard deviation (Means \pm SD). A one-way ANOVA test was used for statistical comparison of the data. Differences between groups were considered significant when $P < .05$. Analyses were carried out using GraphPad Prism Version 7.0 (San Diego, CA).

3. Results

3.1. Generation of DNA integration-free macaque iPSCs and isolation of exosomes

iPSC lines were successfully generated from ear skin fibroblasts (Supplementary Fig. 2a) of four adult male rhesus macaques using DNA integration-free Sendai virus encoding human transcription factors *OCT4*, *SOX2*, *KLF4*, and *c-Myc*. The macaque cells were confirmed as iPSCs by morphology, alkaline phosphatase detection, gene expression, and immunohistochemistry for pluripotency markers as well as teratoma formation in an autologous setting (Fig. 1 and Supplementary Fig. 2a–g) and non-obese diabetes/severe-combined immunodeficient (NOD/SCID) mice [16]. In addition, polymerase chain reaction (PCR) analysis with primers covering the Sendai virus vector confirmed that the macaque iPSC lines were free from integrated external genes (Supplementary Fig. 2h).

Transplantation of macaque iPSCs and collection of their exosomes required feeder-free cell culture conditions. We successfully adapted macaque iPSCs to a feeder-free culture using a widely used murine basement membrane extract (Matrigel™, BD Bioscience) to maintain the cell growth. Pluripotency of the iPSCs cultured under this condition was well maintained.

Exosomes were isolated from the iPSC culture supernatant and characterized by scanning electron microscopy and nanoparticle tracking analysis. The results showed that the exosomes comprised pure spherical vesicles with a diameter of approximately 100 nm (Supplementary Fig. 2i).

3.2. Subcutaneously injected autologous but not allogeneic iPSCs generate teratomas

Each of the four macaques was injected subcutaneously with iPSCs from all four macaques. The cells were premixed with extracellular matrix and injected separately at a bolus of 1×10^7 cells/spot. Autologous iPSCs from all the four macaques generated a teratoma at the injection site within 28 days (Fig. 1a–c). In contrast, none of the 12 injected sites receiving allogeneic iPSCs had a teratoma at 28 days (Fig. 1a and c) and 12 months (data not shown).

3.3. Generation of iPSCs increased the expression of some genetic alleles of MHC Class I and II

Expression of genetic alleles of MHC class I and II were compared between the parental cells (skin fibroblasts used for iPSC induction) and

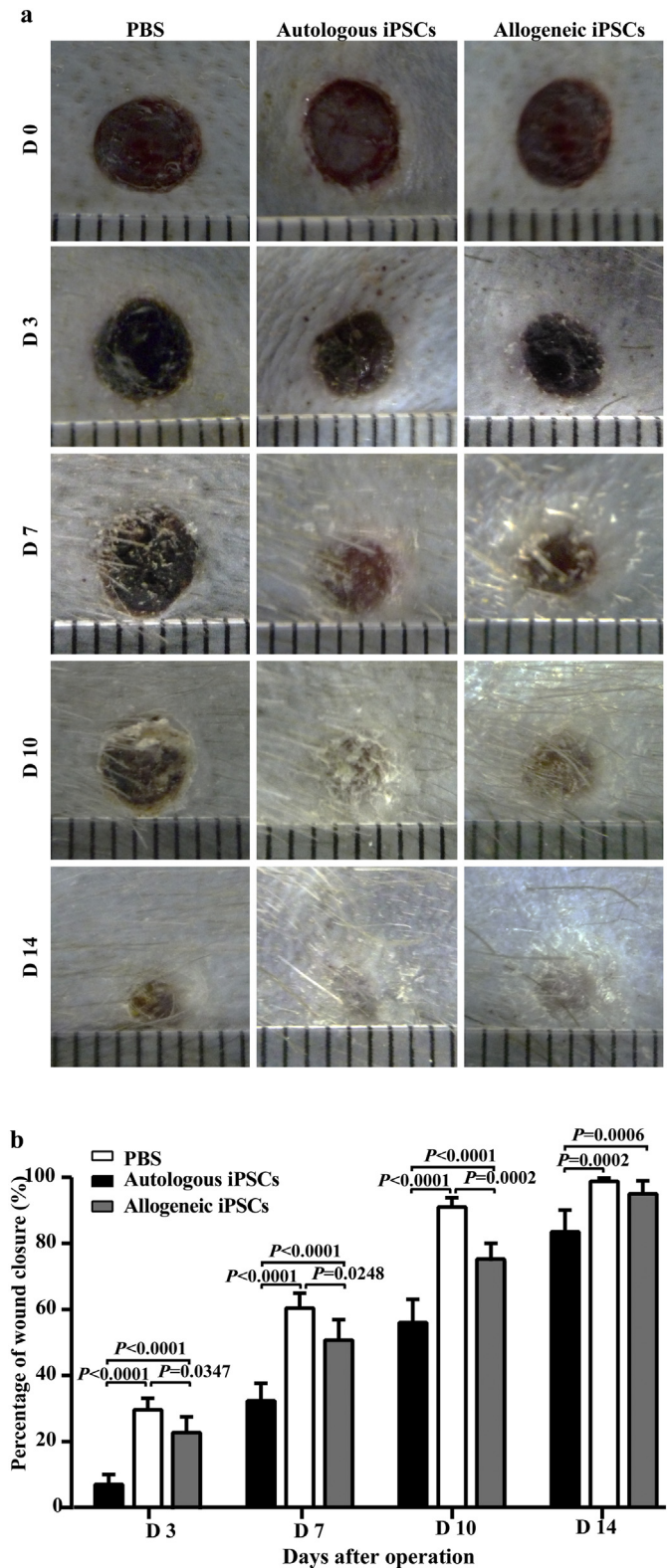


Fig. 2. Macaque iPSCs accelerate wound healing. Wound closure was measured for 14 days. (a) Representative images of wounds treated with PBS, autologous and allogeneic iPSCs on 0, 3, 7, 10, and 14 days after wound punching. (b) Percentages of wound closure. Data represent the means \pm SD. $n = 4$ for autologous and PBS treatments, respectively. $n = 12$ for allogeneic treatment.

iPSCs. In iPSCs, MAMU A and E of MHC class I increased significantly while MAMU B of MHC class I and MAMU DQA, DQB, DRA, DRB, DPA, and DPB of MHC class II were not detectable (Fig. 1d).

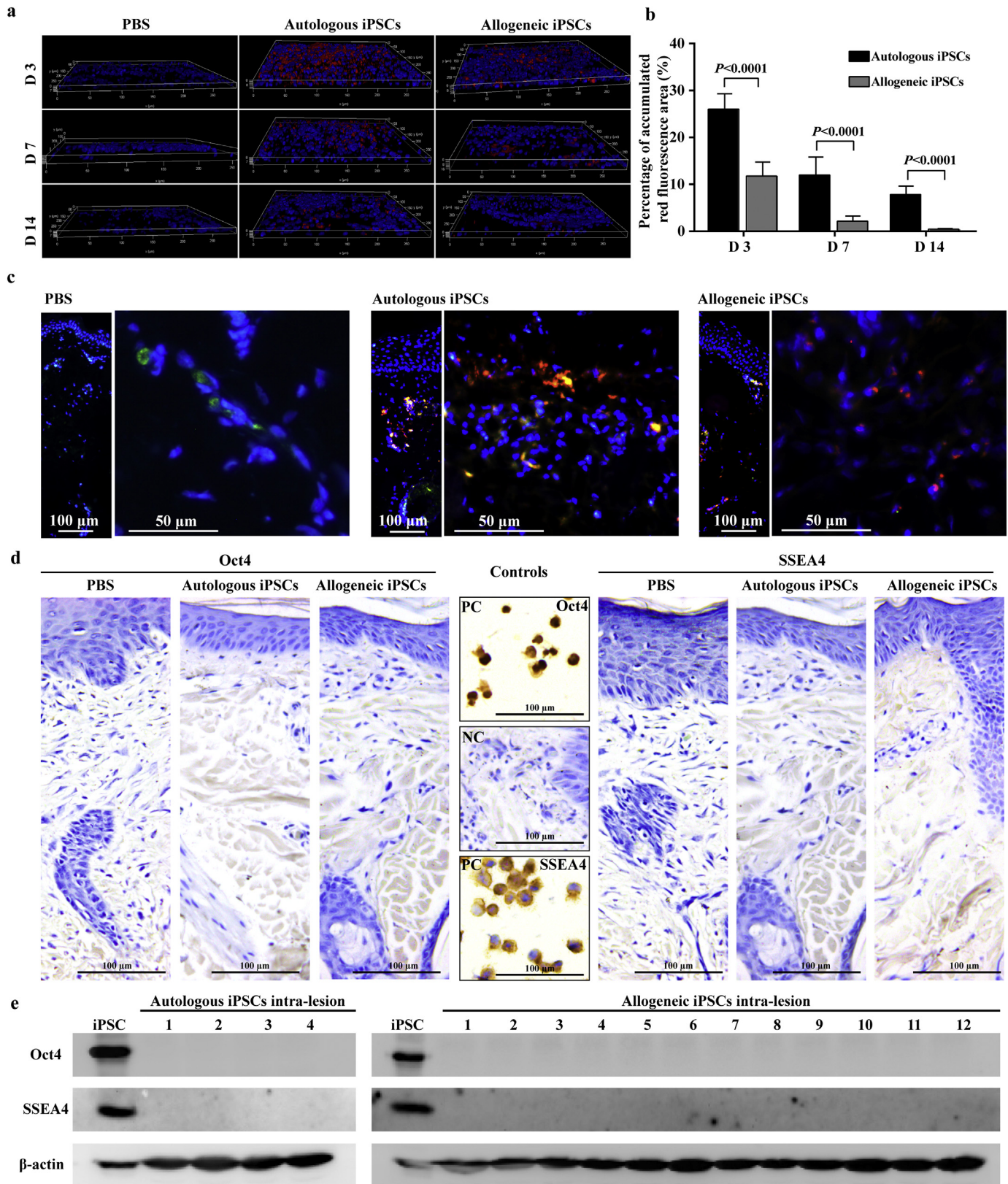


Fig. 3. Transplanted iPSC survival in wounds. (a) Transplanted iPSCs (red) in 3D re-constructed skin wounds by laser confocal microscopy. The layer with the red fluorescent signal was between 7 and 16 μm . (b) Percentage of accumulated area of the red fluorescent signal in the wounds. Data represent the means \pm SD. $n = 4$ for PBS or autologous iPSC treatment. $n = 12$ for allogeneic iPSC treatment. (c) Presence of administered cells (red), newly produced endothelial cells (green), and co-localization of the two (yellow). (d) Absence of pluripotent reprogramming markers (OCT4 and SSEA4) in the skin lesions as demonstrated by immunohistochemistry. Macaque iPSCs smeared on glass slides were used as positive controls. (e) Skin lesions were negative for pluripotency markers (OCT4 and SSEA4), as demonstrated by western blotting; iPSC homogenates served as positive controls. $n = 4$ for autologous iPSC treatment. $n = 12$ for allogeneic iPSC treatment.

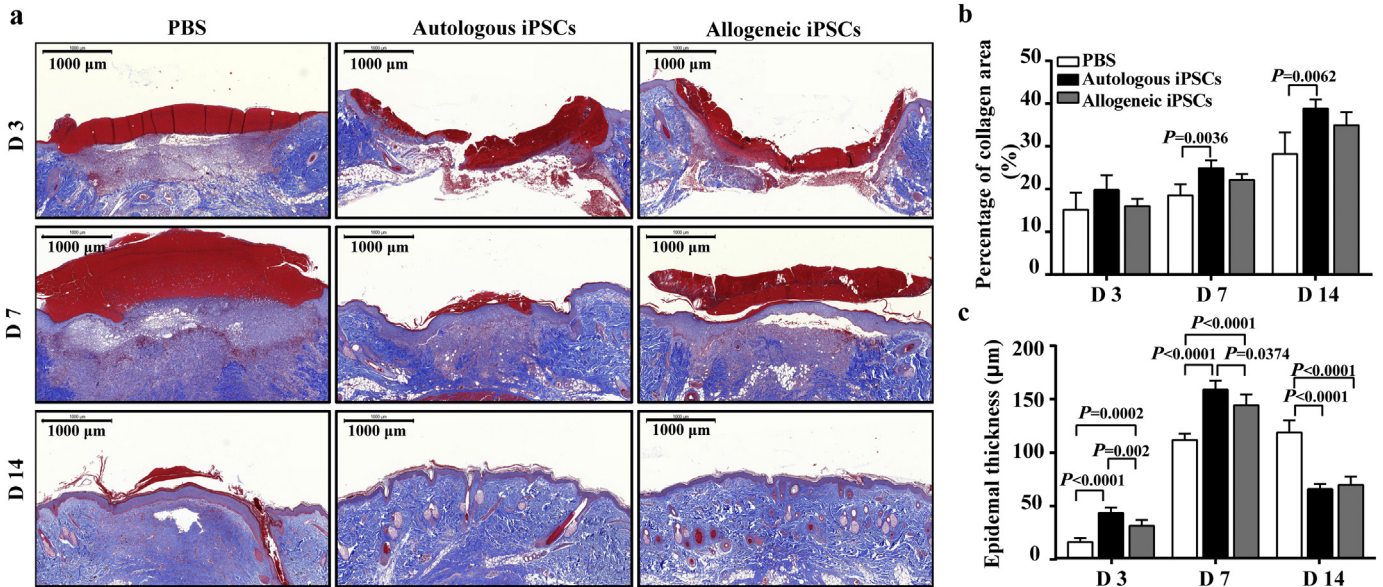


Fig. 4. Macaque iPSCs promote epithelial proliferation and collagen deposition. (a) Representative images of wounds treated with PBS, and autologous and allogeneic iPSCs. Scale bars, 1000 µm. (b) Percentage of collagen area. (c) Epidermal thickness. Data represent the means ± SD. n = 4 for PBS or autologous iPSC treatment. n = 12 for allogeneic iPSC treatment.

3.4. Autologous iPSCs more effectively accelerate wound healing compared to allogeneic iPSCs

The iPSCs were transplanted topically on the rhesus macaque wounds. As shown in Fig. 2, both autologous and allogeneic iPSCs accelerated wound healing compared to that of the PBS control. The percentage of wound closure in the autologous or allogeneic iPSC-treated group was significantly higher than that of animals receiving PBS on day 3, 7, 10, and 14 after transplantation. In addition, the therapeutic effect of autologous iPSCs was significantly better than that of allogeneic iPSCs on day 3, 7, and 10 after transplantation.

3.5. More autologous than allogeneic iPSCs survive in skin wounds

To assess survival, iPSCs were labelled with PKH26 (red fluorescence dye) prior to transplantation. As shown in Fig. 3a and b, by day 7 and 14, a number of cells with red fluorescence were identified in wounds that had received autologous or allogeneic iPSCs, but not in wounds that had received PBS. Significantly more autologous iPSCs than allogeneic iPSCs were detected in the wounds by days 3, 7, and 14.

There was no red fluorescence-positive cell (iPSCs or iPSC-derived cells) in epidermal layer of the wounds on day 14, indicating that the iPSCs did not differentiate into epidermal cells (Fig. 3c). Newly produced endothelial cells represent angiogenesis. CD34 is the marker of such cells. When sections of skin wound tissue were stained with primary antibodies against CD34, along with compatible green fluorescence-labelled secondary antibodies, some of the cells in the lesions that received autologous or allogeneic iPSCs showed colocalization of red and green fluorescence (yellow), indicating that some of the administered iPSCs differentiated into newly produced endothelial cells (Fig. 3c).

3.6. The administered iPSCs lost their pluripotent state in the skin lesions

To determine whether any iPSC remained quiescent in the skin lesion, immunohistochemistry for two pluripotent markers of embryonic cells or iPSCs, namely OCT4 and SSEA4, was performed. Both OCT4 and SSEA4 were found to be negative in the iPSC-treated skin lesions on day 14, as per immunohistochemistry (Fig. 3d) and Western blotting (Fig. 3e) results.

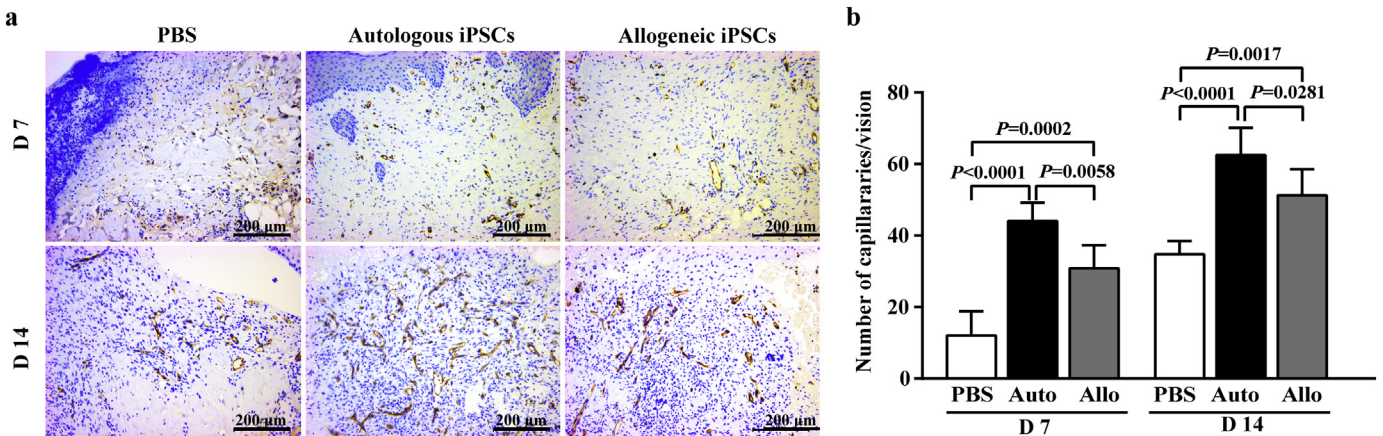


Fig. 5. Macaque iPSCs accelerate angiogenesis in wounds. (a) Representative images of wound sections stained for CD34, a marker of new endothelial cells, on day 7 and 14 after wound punching and PBS, autologous, or allogeneic iPSC treatment. Scale bars = 200 µm. (b) Statistical analyses were performed on numbers of CD34-positive cells per field. Data represent the means ± SD. n = 4 for PBS or autologous iPSC treatment. n = 12 for allogeneic iPSC treatment.

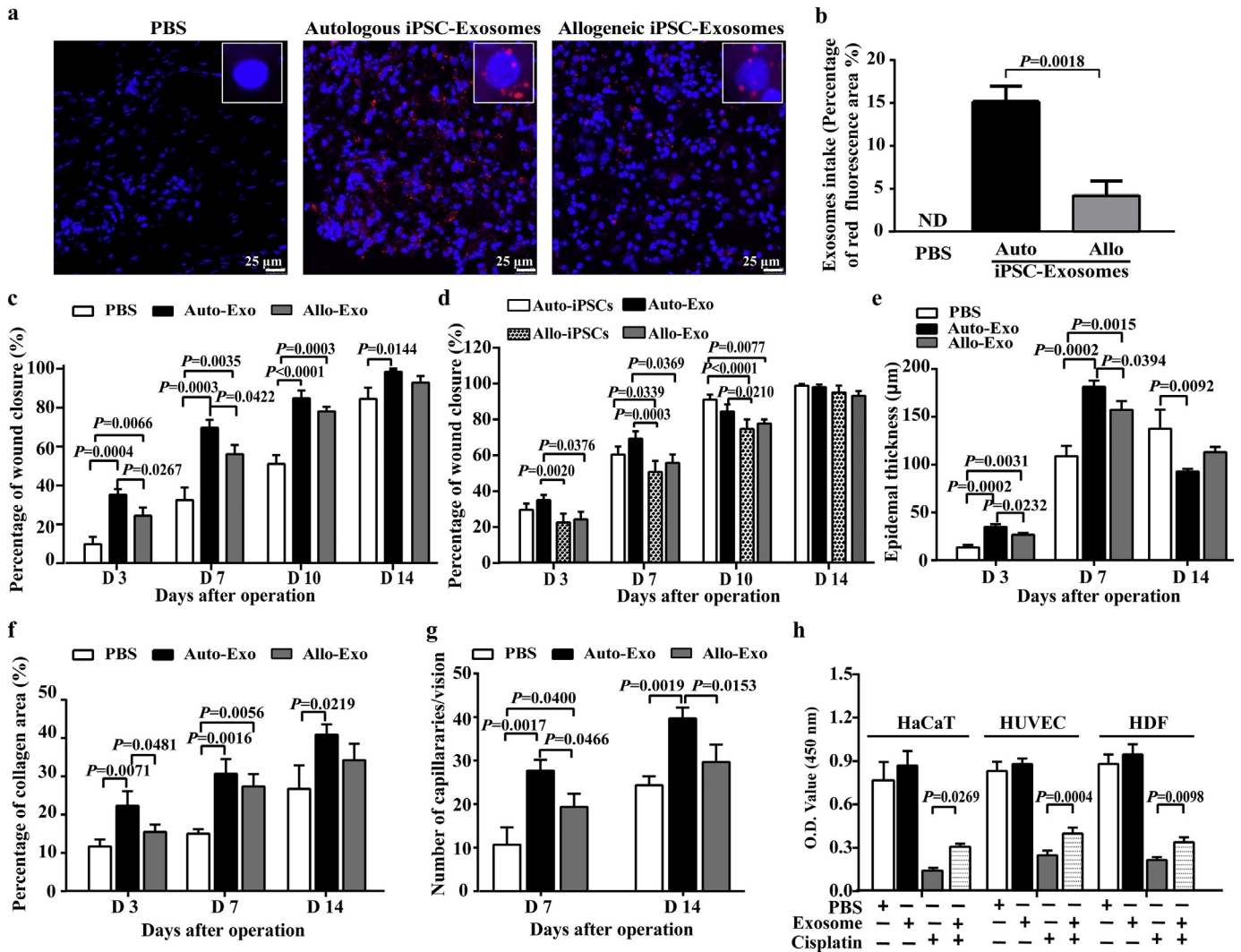


Fig. 6. Macaque iPSC-derived exosomes promote wound healing. (a) iPSC exosomes were labelled with red fluorescent membrane dye (PKH 26) before being topically applied to new punched skin wounds. Representative images of the red fluorescent signal in the wounds at 7 days after exosome application. (b) Percentage of accumulated area of red fluorescent signal in the wounds. (c) Percentages of wound closure. (d) Cross-comparison of wound closure among lesions treated with autologous and allogeneic iPSCs and their exosome counterparts. (e-f) Macaque iPSC-derived exosome therapy promoted epithelial proliferation and collagen deposition as demonstrated by epidermal thickness and the percentage of collagen area out of the whole area observed. (g) Angiogenesis in the wounds. (h) Exosomes promoted cell viability of cisplatin-injured epidermal, endothelial, and skin fibroblastic cells. Data represent the means \pm SD. In panels b-g, $n = 4$ for PBS or autologous iPSC treatment, and $n = 12$ for allogeneic iPSC treatment. In panel h, $n = 4$.

3.7. Autologous iPSCs more effectively accelerate re-epithelialization and collagen deposition in skin wounds compared to allogeneic iPSCs

Masson's trichrome staining showed that wounds developed vascular granulation tissue containing inflammatory cells and fibroblasts. On day 7 after the autologous or allogeneic iPSCs application, the wounds were completely covered by newly formed epithelium, whereas the coverage was incomplete in the PBS groups. On day 7, the newly formed epithelial layer was significantly thicker on the autologous iPSC-treated wounds ($158.8 \pm 8.526 \mu\text{m}$) than that on allogeneic iPSC-treated wounds ($144.5 \pm 10.04 \mu\text{m}$), with both being thicker than that on the PBS-treated wounds ($111.8 \pm 5.997 \mu\text{m}$). However, on day 14, the epithelial layers on the autologous iPSC-treated wounds ($66.0 \pm 4.678 \mu\text{m}$) and allogeneic iPSC-treated wounds ($69.8 \pm 6.298 \mu\text{m}$) were significantly thinner than that on the PBS-treated wounds ($118.9 \pm 11.5 \mu\text{m}$) (Fig. 4).

Compared to the PBS control, both autologous and allogeneic iPSCs significantly increased collagen deposition in the wounds on day 3, 7, and 14. The differences between autologous and allogeneic iPSCs were significant on days 3 and 7 but not on day 14, with the alignment of

collagen fibres more organized in wounds treated with autologous iPSCs (Fig. 4).

3.8. Autologous iPSCs more effectively promote angiogenesis in skin wounds compared to allogeneic iPSCs

By day 7 and 14 of wound healing, the numbers of CD34-positive capillaries in autologous and allogeneic iPSC-treated wounds were significantly higher than those in wounds treated with PBS. Furthermore, significant difference was observed between wounds treated with autologous and allogeneic iPSCs (Fig. 5).

3.9. Wounds treated with autologous iPSCs were morphologically more similar to normal skin than those treated with allogeneic iPSCs

Surprisingly, all healed wounds had hair, as shown in Fig. 2. Wounds treated with autologous iPSCs were morphologically better than those treated with allogeneic iPSCs. The former became similar to normal skin, upon healing, on day 14. This phenomenon was verified by sectioning the whole paraffin block and staining the sections at an interval

of 4 sections. Sections cut through the centre of the lesion were used for immunohistochemistry or Masson's trichrome staining (Fig. 3d and 4a).

3.10. More autologous than allogeneic iPSC exosomes are detected inside cells of skin wounds

Exosomes were also labelled with PKH26 (red fluorescence) prior to being applied to the wound surface. Both autologous and allogeneic exosomes were detected inside cells of the skin wounds on day 3. The up-taken of autologous exosomes was significantly higher than that of the allogeneic exosomes (Fig. 6a and b).

3.11. Autologous iPSC exosomes are more effectively accelerate wound healing, epithelisation, and angiogenesis compared to allogeneic iPSC exosomes

Similar to iPSCs, both autologous and allogeneic iPSC exosomes accelerated wound closure when compared to the PBS control. The autologous iPSC exosomes were more efficient than allogeneic iPSC exosomes (Fig. 6c, Supplementary Fig. 3a). Although there were no statistically significant differences in wound closure speed between autologous iPSCs and their exosomes or between allogeneic iPSCs and their exosomes (Fig. 6d), morphological examination on day 14 showed that lesions treated with autologous iPSC exosomes were like a typical healed skin (Supplementary Fig. 3b) while those treated with autologous iPSCs looked similar to a normal skin (Fig. 4a).

In particular, the exosomes promoted epithelisation. Thicknesses of epithelial layer were 181.4 ± 6.54 , 157.2 ± 9.407 and 108.9 ± 10.75 μm in the autologous iPSC exosome, allogeneic iPSC exosome, and PBS groups, respectively, on day 7 (Fig. 6e and Supplementary Fig. 3b). Autologous exosomes were most effective. On day 14, the epithelial layer on wounds treated with autologous iPSC exosomes was most significantly remodelled. The effect of these exosomes on collagen deposition was similar to that on epithelisation (Fig. 6f and Supplementary Fig. 3b).

The exosomes also promoted angiogenesis in the wounds. The number of CD34-positive capillaries in wounds treated with autologous iPSC exosomes was significantly more than that in wounds treated with allogeneic iPSC exosomes or PBS on both day 7 and 14. The effect of allogeneic iPSC exosomes was significantly better than that of PBS on day 7 (Fig. 6g and Supplementary Fig. 3c).

3.12. Exosomes increased cell viability of injured epidermal, endothelial, and fibroblastic cells

Exosomes isolated from the four rhesus macaques were separately used to treat the cells. While they did not affect the viability of the cells without any harmful treatment, they significantly increased viability of cisplatin-injured epidermal, endothelial, and fibroblastic cells (Fig. 6h).

3.13. Either autologous or allogeneic iPSC exosomes induced pluripotency in exosome-receiving cells

The exosomes isolated from all four monkey iPSC lines were negative for pluripotent reprogramming markers (OCT4, SOX2, KLF4, and c-Myc), and positive for exosome markers (TSG101 and ALIX) (Fig. 7a). Either of autologous or allogeneic exosome-treated skin lesions on day 14 was positive for pluripotency markers (OCT4 and SSEA4), as demonstrated by immunohistochemistry (Fig. 7b) and Western blotting (Fig. 7c).

iPSC exosomes contained mRNAs of pluripotency markers OCT4, SOX2, KLF4, and Nanog. The mRNA levels of pluripotency markers in iPSC exosomes were significantly lower than those in iPSCs (Fig. 7d).

OCT4, SOX2, KLF4, and Nanog mRNA levels in fibroblastic cells treated with iPSC exosomes for 16 h were 2.75, 1.82, 1.55, and 3.73 fold of those in fibroblastic cells without exosome treatment,

respectively. As positive controls, the mRNA levels in iPSCs were 2830.62, 14.16, 25.78, and 31.51 fold of those in fibroblastic cells without exosome treatment, respectively. The mRNA levels of OCT4, SOX2, KLF4, and Nanog in fibroblastic cells harvested 4 h after iPSC exosome incubation were 5.78, 3.01, 8.54, and 3.37 times of those in fibroblastic cells harvested 16 h after incubation (Fig. 7e).

Some fibroblastic cells were incubated in iPSC exosome-containing medium for 4 h followed by iPSC exosome-free medium for 12 h, or in iPSC exosome-containing medium for 16 h followed by iPSC exosome-free medium for 24 h. Compared to the cells harvested at 4 h or 16 h after iPSC exosome incubation, those incubated 4 h with exosomes followed by 12 h without exosomes, or 16 h with exosomes followed by 24 h without exosomes showed decreased levels of pluripotent factor mRNAs (close to 1), similar to those without iPSC exosome treatment from the beginning (= 1) (Fig. 7e).

None of the iPSC exosome-treated fibroblastic cells was positive for pluripotent factors (Fig. 7g). The negative result was confirmed by Western blotting (Fig. 7f). Serving as positive controls, both immunofluorescence staining and Western blotting confirmed that iPSCs contained significant amount of pluripotent factor proteins (Fig. 7g and f).

3.14. Subcutaneously injected allogeneic, but not autologous, iPSCs generated host immune response

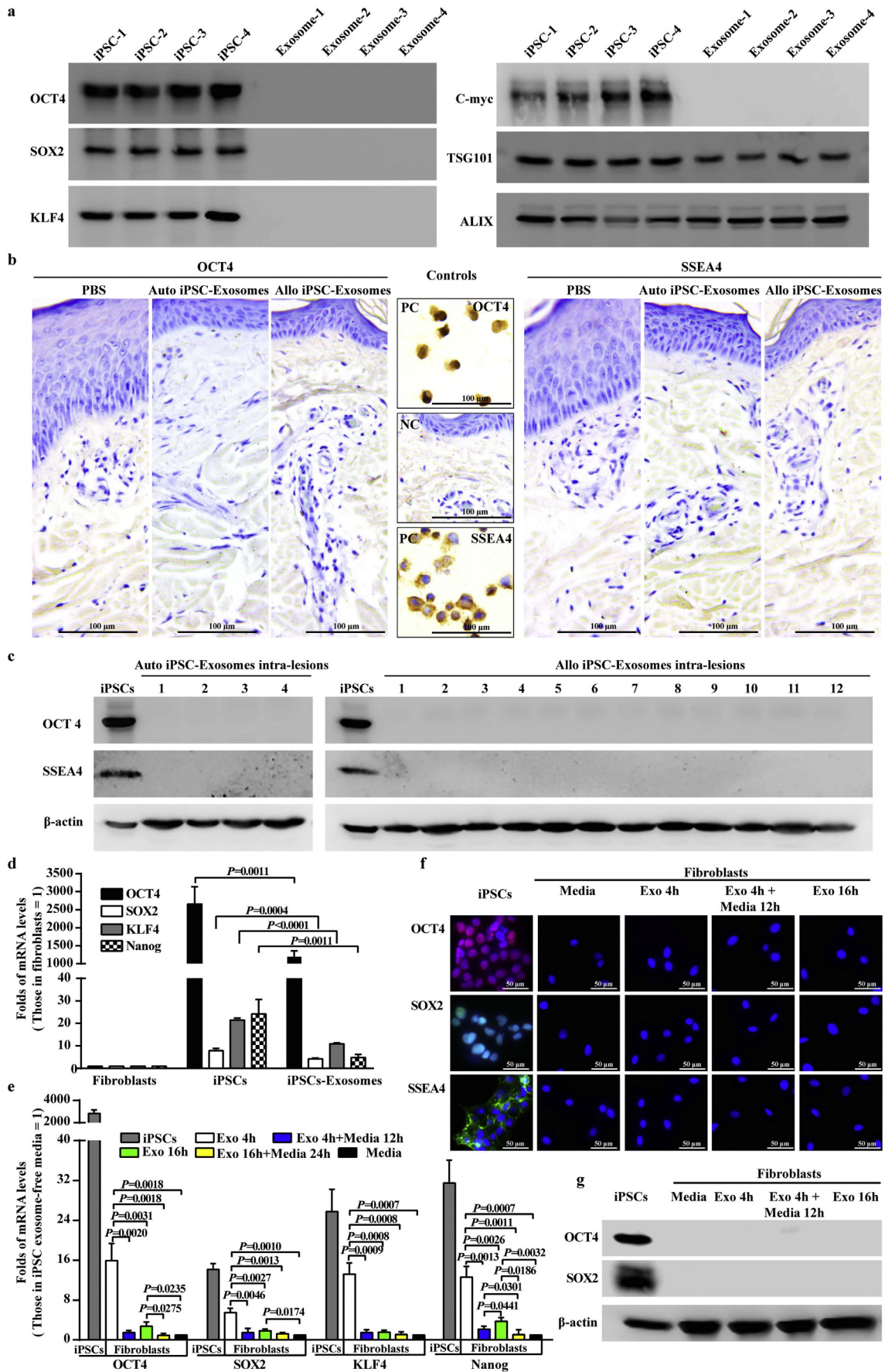
To determine whether an immune response is generated to autologous or allogeneic iPSCs, cells were injected subcutaneously, as in case of the teratoma formation, 2 months after the teratoma assay. Injection site and surrounding tissues were collected 3 days after iPSC injection. Western blotting showed that all the allogeneic iPSC-containing tissues, but none of the autologous iPSC containing tissues, were positive for the pan T lymphocyte marker CD3 and B lymphocyte maker CD20 (Fig. 8a). In the meantime, all the allogeneic iPSC-treated lesions, but none of the autologous iPSC treated lesions, were positive for CD3 and CD20 (Fig. 8b). All tissues containing subcutaneously injected exosomes or skin lesions containing topically delivered exosomes were negative for CD3 and CD20 (Fig. 8c). Monocyte/macrophage marker CD68 was negative in all samples (Fig. 8a–c).

3.15. iPSC-treated wounds do not develop teratoma

None of the rhesus macaques developed teratoma in the wounds (Fig. 2a and Supplementary Fig. 3a).

4. Discussion

Immunogenicity needs to be evaluated before considering iPSCs and their derivatives for experimental or clinical application [27]. Zhao et al. failed in generating teratomas using inbred syngeneic mouse iPSC lines, and identified nine genes that may be responsible for the rejection of syngeneic mouse iPSCs [5]. In support of these findings, de Almeida et al. have also reported the rejection of mouse iPSC lines [6]. However, Araki et al. subsequently claimed that inherent immunogenicity in murine embryonic stem cell (mESC), syngeneic mouse iPSC lines, and their cellular derivatives was negligible, although they also found T cell infiltration in engrafted cardiomyocytes, with the size of teratomas in wild-type C57BL/6 animals being slightly smaller than that in SCID mice [13]. In addition, Strnadel et al. examined the survival of syngeneic and allogeneic iPSC-derived neural precursors after spinal grafting in inbred minipigs [7]. They found the lack of immunogenicity of iPSC-derived neural precursor cells engrafted into the naïve non-injured or spinal trauma-injured spinal cord. Moreover, successful engraftment was observed in inbred allogeneic minipigs receiving only time-limited immunosuppression. However, the comparison of immune reaction between recipients has not yet advanced to assessment of that between the same animal receiving autologous and allogeneic iPSCs and their derivatives, nor to that in a model of non-human primates, with the latter being



especially important because it is the most closely model for potential human clinical application.

Host immune response does not necessarily translate into immune rejection. If the heterogenic antigens comprise intracellular proteins, rather than secreted proteins or membrane proteins with extracellular profiles, minimal opportunities exist for the immune system to contact the antigens when the cells are alive. Moreover, an immune response raised by intracellular antigens released from dead cells does not have the chance to reach their targeted intracellular antigens while the cells remain alive. Thus, the best approach to test whether iPSCs can survive beyond an incompletely differentiated stage *in vivo* is to utilize a teratoma assay in immunocompetent animals. In the present study, iPSC lines from four different monkey consanguineal families were used to tested teratoma formation. All four monkeys subcutaneously injected with autologous iPSCs generated teratomas in 100% of the injection sites, whereas none of the monkeys generated teratomas in sites injected with allogeneic iPSCs. The result showed that, in all 12 cross-evaluation combinations, non-inbred allogeneic primate iPSCs do not survive for a long time. Subsequently, to demonstrate whether the initial injection generated immune response, secondary injection of the iPSCs was performed. The injected cells and surrounding tissue were harvested three days after injection to avoid the presence of iPSC-derived lymphocytes. These results further confirmed that the monkeys developed an immune response to all non-inbred allogeneic iPSCs, demonstrated by the infiltration of CD3- and CD20-positive cells. Neither autologous nor allogeneic iPSCs, nor their exosomes, caused innate immune response, as demonstrated by the absence of macrophage in iPSC- or exosome-receiving tissue.

Wound healing constitutes an integrated and well-coordinated chain of events that involves interactions among different cells, extracellular matrix molecules, soluble mediators, and cytokines [28]. Numerous types of stem cells and their derivatives represent candidates for stem cell therapy, with each exhibiting distinct advantages and disadvantages. For example, MSCs are most commonly tested *in vivo*. Studies have shown that local or systematic administration of MSCs [24] and endothelial progenitor cells [29] improve wound closure. However, preparing the appropriate number of personalized MSCs or endothelial progenitor cells is extremely challenging [3]. In comparison, iPSCs comprise an abundant and malleable source with enhanced differentiation potential for cell therapy, which may overcome this hurdle [3,30]. Requiring generation only once in a lifetime, unlimited numbers of personalized iPSCs can be prepared and stored for all future applications. For example, in the present study, we showed that topically administered iPSCs accelerated healing of full-thickness skin wounds in monkeys. Although both autologous and allogeneic iPSCs were effective, more autologous iPSCs survived in the wound, thereby enhancing overall efficacy. Notably, all healed wounds had hair. Wounds treated with autologous iPSCs looked similar to normal skin on day 14; this could possibly be due to the small size of wound (only 4 mm in diameter).

Wound healing requires angiogenesis to bring nutrition to the cells, deposition of extracellular matrix tissue to replace tissue loss, and epithelial proliferation to restore the boundary between the body and its environment. Through histological examination, we demonstrated that capillary number, collagen deposition, and the thickness of the epithelial layer in the wounds were increased significantly by iPSC-treatment compared with treatment with PBS before day 10. By day 14, the epithelial thickness in autologous iPSC-treated wounds had virtually been remodelled and returned to normal, whereas thickness in

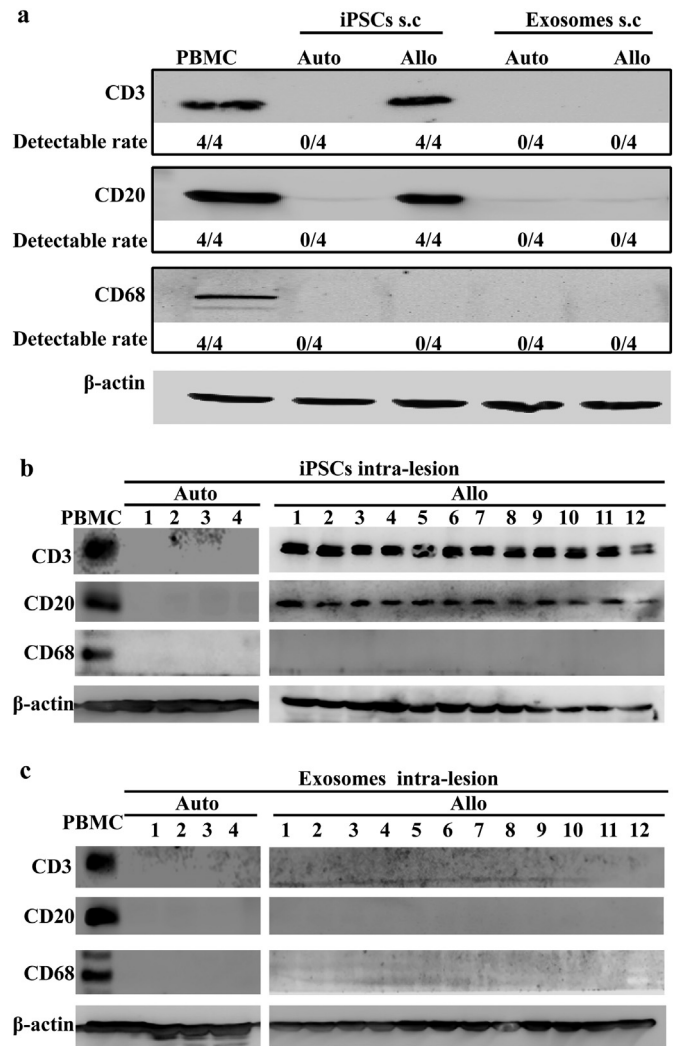


Fig. 8. Effects of autologous and allogeneic iPSCs and their exosomes on infiltration of immune cells. (a) Presence of CD3, CD20, and CD68 proteins in iPSC- or exosome-containing skin. Western blot images and the detectable rates of corresponding markers are presented. Protein of autologous peripheral blood mononuclear cells served as positive control. (b-c) Presence of CD3, CD20, and CD68 proteins in skin lesions three days after iPSC or exosome treatment. The membranes were over-exposed to avoid false negative result.

PBS- or allogeneic iPSC-treated wounds was still increasing. There was no difference in collagen deposition among groups by day 14. Notably, the time frames of these parameters matched the timing of non-intervened wound closure. Consistent with wound closure, autologous iPSCs were more effective than allogeneic iPSCs in promoting epithelial recovery, angiogenesis, and collagen deposition.

Stem cells promote tissue repair and regeneration by providing functional parenchymal cells, promoting angiogenesis, and secreting beneficial substances. Absence of administered iPSCs in the epidermal layer indicated that their transformation into epidermal cells is not the mechanism underlying promoting skin wound healing. Rather, co-localization of labelling signals of some administered cells and new endothelial cells demonstrated that some of the administered cells

Fig. 7. Macaque iPSC-derived exosomes did not induce pluripotency of host cells in skin lesions. (a) The exosomes were negative for pluripotent reprogramming markers (OCT4, SOX2, KLF4, and c-Myc), and positive for exosome markers (TSG101 and ALIX) as shown by western blotting. (b) Host cells in skin lesions were negative for pluripotency markers (OCT4 and SSEA4), as demonstrated by immunohistochemistry. Macaque iPSCs, smeared on glass slides, were used as positive controls. (c) Skin lesions were negative for pluripotency markers (OCT4 and SSEA4), as demonstrated by western blotting. Homogenate of iPSCs served as positive controls; $n = 4$ for autologous iPSC treatment; $n = 12$ for allogeneic iPSC treatment. (d) OCT4, SOX2, KLF4, and Nanog mRNA levels in fibroblastic cells, iPSCs, and iPSC-derived exosomes. (e) OCT4, SOX2, KLF4, and Nanog mRNA levels in fibroblastic cells treated with iPSC exosome-containing medium or exosome-free medium. mRNAs from iPSCs served as positive controls. Immunofluorescence staining (f) and Western blotting (g) of fibroblastic cells treated with iPSC exosome-containing medium and iPSCs. Exo 4 h and Exo 16 h represent cells incubated with exosome-containing medium for 4 h and 16 h, respectively. Media represent cells incubated in iPSC exosome-free medium. $n = 3$.

differentiated into endothelial cells and participated in promoting angiogenesis.

iPSC-secreted exosomes represent a functional natural source of therapeutic substances, carrying a complex cargo of proteins, lipids, and nucleic acids [31–33]. Exosomes from embryonic, mesenchymal, and hematopoietic stem cells exert beneficial effects on different exosome-receiving cells by acting as mediators of cell-to-cell communication [17,34–36]. Numerous functionally cooperative proteins are simultaneously packed and delivered by exosomes, allowing co-functionality. In addition, such cargo is protected by a biomembrane [37], rendering them less accessible to enzymes and other materials that can destroy proteins. Therefore, exosome-packaged proteins are more stable and efficient than individually secreted proteins.

Despite having strategies to reduce the risk of teratoma formation following iPSC transplantation, the risk of forming teratomas remains a concern for therapeutic applications of iPSCs and iPSC-derived differentiated cells [38]. Using 53 experimental conditions and disease models, we recently demonstrated that intravenously or topically disseminated iPSCs do not form teratoma; the injected iPSCs do not differentiate into long-lasting stromal cells, such as neural and myocardial cells, and lose pluripotency within 3 days *in vivo* [16]. In the present study, no teratoma was found in the iPSC-administered skin wounds, and no administered cell remained in pluripotent state after 14 days of administration. Exosomes released from iPSCs are not expected to transform into teratoma, since they are chromosome-free. However, cells selectively sorted a fraction of different types of cellular proteins in different amounts into exosomes [31]. We found that common pluripotent factors such as OCT4, SOX2, KLF4, and c-Myc were not sorted into exosomes, thereby diminishing the possibility that iPSCs transferred pluripotency to other cells through exosomes. Another possible mechanism of transferring pluripotency through exosomes is via exosomes carrying mRNAs of pluripotent factors. Khan et al. reported the presence of mRNAs of pluripotent factors in fibroblastic cells harvested 24 h after incubation with exosomes obtained from mouse embryonic stem cells [17]. We did find low levels of mRNAs of pluripotent factors in iPSC-secreted exosomes. The presence of these mRNAs in exosome-receiving cells was transient, and the transferred mRNAs were not sufficient to be translated into detectable amount of proteins of pluripotent factors. Furthermore, neither autologous nor allogeneic exosomes were found to induce the expression of stem cell markers in exosome-receiving tissue or cells. Thus, our results confirmed that exosomes carry no risk of forming teratomas. iPSC-derived exosomes may constitute a promising alternative to intact iPSC therapy. When the effect of iPSCs and their exosomes were compared, there was no statistically significant difference in wound closure speed between autologous iPSCs and their exosomes or between allogeneic iPSCs and their exosomes, although morphological examination on day 14 showed that lesions treated with autologous iPSCs were more similar to normal skin than those treated with autologous iPSC exosomes. This result indicated that exosome is one of the major participants by which iPSCs promote wound healing.

In addition, autologous and allogeneic iPSC exosomes were compared with regard to skin wound healing in monkeys that had previously received two subcutaneous injections of intact iPSCs for observations of teratoma formation and immunogenicity. Although fewer allogeneic iPSC exosomes were uptaken by cells in the wounds than autologous iPSC exosomes, and were not as effective as intact iPSCs and autologous iPSC exosomes, allogeneic iPSC exosomes were considered sufficiently effective in accelerating wound healing. We also demonstrated that exosomes promote the viability of epidermal, endothelial, and fibroblastic cells, the three major cells responsible for skin wound healing. Considering the advantages of mass-production, potential for using higher dosage, and lack of teratoma formation, allogeneic iPSC exosomes may thus represent the product of choice among autologous and allogeneic iPSCs and their derivatives for

promoting skin wound healing. Accordingly, may become the next “off-the shelf” cell-free product for wound healing.

In summary, we showed that both autologous and allogeneic iPSCs as well as their exosomes accelerated the healing of full-thickness skin wounds in the rhesus macaque. Allogeneic iPSCs were attacked by the immune system and, along with their exosomes, were less effective compared to their autologous counterparts. Nevertheless, allogeneic iPSC exosomes could constitute the next “off-the shelf” product for wound healing owing to their cell-free nature and potential for mass production.

Supplementary data to this article can be found online at <https://doi.org/10.1016/j.ebiom.2019.03.011>.

Acknowledgements

We thank Weizhi Ji and Tianqing Li, along with Jingjing He and Shumei Zhao from Kunming University of Science and Technology for the gift of monkey ESCs and assistance in optimizing the condition of monkey iPSC culture, respectively. We also appreciate the assistance of the Shanghai Public Health Clinical Centre for animal care.

Funding sources

This study was supported by the Great Research Plan Program (91539120 to S.C.), Key International Cooperation Program (81220108002 to S.C.) and General Program (81470260 to M.X.) of the National Natural Science Foundation of China, and the National Key R&D Program of China (2016YFC1305101 to S.C.).

Declaration of interests

The authors declare no competing financial interests.

Author contributions

Conceptualization, S.C.; Methodology, M.L., P.L., M.X., X.W., Y.L., X.W., D.M., and N.S.; Investigation, M.L., X.W., and M.X.; Writing – Original Draft, S.C., M.X., and M.L.; Writing – Review & Editing, M. X. and S.C.; Funding Acquisition, S.C.

References

- [1] Howden SE, Thomson JA, Little MH. Simultaneous reprogramming and gene editing of human fibroblasts. *Nat Protoc* 2018;13:875–98.
- [2] Chari S, Mao S. Timeline: iPSCs—the first decade. *Cell* 2016;164:580.
- [3] Robinton DA, Daley GQ. The promise of induced pluripotent stem cells in research and therapy. *Nature* 2012;481:295–305.
- [4] Zhao T, Zhang ZN, Westenskow PD, Todorova D, Hu Z, Lin T, et al. Humanized mice reveal differential immunogenicity of cells derived from autologous induced pluripotent stem cells. *Cell Stem Cell* 2015;17:353–9.
- [5] Zhao T, Zhang ZN, Rong Z, Xu Y. Immunogenicity of induced pluripotent stem cells. *Nature* 2011;474:212–5.
- [6] de Almeida PE, Meyer EH, Kooreman NG, Diecke S, Dey D, Sanchez-Freire V, et al. Transplanted terminally differentiated induced pluripotent stem cells are accepted by immune mechanisms similar to self-tolerance. *Nat Commun* 2014;5:3903.
- [7] Strnadel J, Carromeu C, Bardy C, Navarro M, Platoshyn O, Glud AN, et al. Survival of syngeneic and allogeneic iPSC-derived neural precursors after spinal grafting in minipigs. *Sci Transl Med* 2018;10.
- [8] Tapia N, Scholer HR. Molecular obstacles to clinical translation of iPSCs. *Cell Stem Cell* 2016;19:298–309.
- [9] Morizane A, Doi D, Kikuchi T, Okita K, Hotta A, Kawasaki T, et al. Direct comparison of autologous and allogeneic transplantation of iPSC-derived neural cells in the brain of a non-human primate. *Stem Cell Reports* 2013;1:283–92.
- [10] Hong SG, Lin Y, Dunbar CE, Zou J. The role of nonhuman primate animal models in the clinical development of pluripotent stem cell therapies. *Mol Ther* 2016;24:1165–9.
- [11] French A, Yang CT, Taylor S, Watt SM, Carpenter L. Human induced pluripotent stem cell-derived B lymphocytes express sIgM and can be generated via a hemogenic endothelium intermediate. *Stem Cells Dev* 2015;24:1082–95.
- [12] Kooreman NG, Kim Y, de Almeida PE, Termglinchan V, Diecke S, Shao NY, et al. Autologous iPSC-based vaccines elicit anti-tumor responses *in vivo*. *Cell Stem Cell* 2018;22:501–13 e7.

- [13] Araki R, Uda M, Hoki Y, Sunayama M, Nakamura M, Ando S, et al. Negligible immunogenicity of terminally differentiated cells derived from induced pluripotent or embryonic stem cells. *Nature* 2013;494:100–4.
- [14] Guha P, Morgan JW, Mostoslavsky G, Rodrigues NP, Boyd AS. Lack of immune response to differentiated cells derived from syngeneic induced pluripotent stem cells. *Cell Stem Cell* 2013;12:407–12.
- [15] Chhabra A. Inherent immunogenicity or lack thereof of pluripotent stem cells: implications for cell replacement therapy. *Front Immunol* 2017;8:993.
- [16] Meng Xiang ML, Quan Jing, Ming Xu, Meng Dan, Cui Anfeng, Li Ning, et al. Direct in vivo application of induced pluripotent stem cells is feasible and can be safe. *Theranostics* 2019;9:290–310.
- [17] Khan M, Nickoloff E, Abramova T, Johnson J, Verma SK, Krishnamurthy P, et al. Embryonic stem cell-derived exosomes promote endogenous repair mechanisms and enhance cardiac function following myocardial infarction. *Circ Res* 2015;117:52–64.
- [18] Mathiyalagan P, Liang Y, Kim D, Misener S, Thorne T, Kamide CE, et al. Angiogenic mechanisms of human CD34(+) stem cell exosomes in the repair of ischemic hindlimb. *Circ Res* 2017;120:1466–76.
- [19] Daadi MM, Barberi T, Shi Q, Lanford RE. Nonhuman primate models in translational regenerative medicine. *Stem Cells Dev* 2014;23(Suppl. 1):83–7.
- [20] Hallett PJ, Deleidi M, Astradsson A, Smith GA, Cooper O, Osborn TM, et al. Successful function of autologous iPSC-derived dopamine neurons following transplantation in a non-human primate model of Parkinson's disease. *Cell Stem Cell* 2015;16:269–74.
- [21] Armstrong DG, Boulton AJM, Bus SA. Diabetic foot ulcers and their recurrence. *N Engl J Med* 2017;376:2367–75.
- [22] Linard C, Brachet M, Strup-Perrot C, L'Homme B, Busson E, Squiban C, et al. Autologous bone marrow mesenchymal stem cells improve the quality and stability of vascularized flap surgery of irradiated skin in pigs. *Stem Cells Transl Med* 2018;7:569–82.
- [23] Driskell RR, Lichtenberger BM, Hoste E, Kretschmar K, Simons BD, Charalambous M, et al. Distinct fibroblast lineages determine dermal architecture in skin development and repair. *Nature* 2013;504:277–81.
- [24] Daley GQ. The promise and perils of stem cell therapeutics. *Cell Stem Cell* 2012;10:740–9.
- [25] Polo JM, Liu S, Figueroa ME, Kulalert W, Eminli S, Tan KY, et al. Cell type of origin influences the molecular and functional properties of mouse induced pluripotent stem cells. *Nat Biotechnol* 2010;28:848–55.
- [26] Jiang L, Yin M, Wei X, Liu J, Wang X, Niu C, et al. Bach1 represses Wnt/beta-catenin signaling and angiogenesis. *Circ Res* 2015;117:364–75.
- [27] Kaneko S, Yamanaka S. To be immunogenic, or not to be: that's the iPSC question. *Cell Stem Cell* 2013;12:385–6.
- [28] Valacchi G, Zanardi I, Sticozzi C, Bocci V, Travagli V. Emerging topics in cutaneous wound repair. *Ann N Y Acad Sci* 2012;1259:136–44.
- [29] Liu ZJ, Velazquez OC. Hyperoxia, endothelial progenitor cell mobilization, and diabetic wound healing. *Antioxid Redox Signal* 2008;10:1869–82.
- [30] Hockemeyer D, Jaenisch R. Induced pluripotent stem cells meet genome editing. *Cell Stem Cell* 2016;18:573–86.
- [31] Choi DS, Kim DK, Kim YK, Gho YS. Proteomics of extracellular vesicles: exosomes and ectosomes. *Mass Spectrom Rev* 2015;34:474–90.
- [32] Gezer U, Ozgur E, Cetinkaya M, Isin M, Dalay N. Long non-coding RNAs with low expression levels in cells are enriched in secreted exosomes. *Cell Biol Int* 2014;38:1076–9.
- [33] Huber HJ, Holvoet P. Exosomes: emerging roles in communication between blood cells and vascular tissues during atherosclerosis. *Curr Opin Lipidol* 2015;26:412–9.
- [34] Ong SG, Lee WH, Huang M, Dey D, Kodo K, Sanchez-Freire V, et al. Cross talk of combined gene and cell therapy in ischemic heart disease: role of exosomal microRNA transfer. *Circulation* 2014;130:S60–9.
- [35] Tao SC, Yuan T, Zhang YL, Yin WJ, Guo SC, Zhang CQ. Exosomes derived from miR-140-5p-overexpressing human synovial mesenchymal stem cells enhance cartilage tissue regeneration and prevent osteoarthritis of the knee in a rat model. *Theranostics* 2017;7:180–95.
- [36] Vandergriff A, Huang K, Shen D, Hu S, Hensley MT, Caranasos TG, et al. Targeting regenerative exosomes to myocardial infarction using cardiac homing peptide. *Theranostics* 2018;8:1869–78.
- [37] Tickner JA, Urquhart AJ, Stephenson SA, Richard DJ, O'Byrne KJ. Functions and therapeutic roles of exosomes in cancer. *Front Oncol* 2014;4:127.
- [38] Ben-David U, Benvenisty N. The tumorigenicity of human embryonic and induced pluripotent stem cells. *Nat Rev Cancer* 2011;11:268–77.